Received: 16 April 2021 | Accepted: 14 December 2021

DOI: 10.1111/gcb.16077

Global Change Biology WILEY

RESEARCH ARTICLE

Global divergent trends of algal blooms detected by satellite during 1982–2018

Chong Fang[1,2] | Kaishan Song[1,3] | Hans W Paerl[4,5] | Pierre-Andre Jacinthe[6] | Zhidan Wen[1] | Ge Liu[1] | Hui Tao[1,7] | Xiaofeng Xu[8] | Tiit Kutser[9] | Zongming Wang[1] | Hongtao Duan[10] | Kun Shi[10] | Yingxin Shang[1] | Lili Lyu[1,7] | Sijia Li[1] | Qian Yang[11] | Dongmei Lyu[11] | Dehua Mao[1] | Baohua Zhang[3] | Shuai Cheng[3] | Yunfeng Lyu[12]

[1]Northeast Institute of Geography and Agroecology, CAS, Changchun, China

[2]Faculty of infrastructure engineering, Dalian University of Technology, Dalian, China

[3]School of Environment and Planning, Liaocheng University, Liaocheng, China

[4]Institute of Marine Sciences, University of North Carolina at Chapel Hill, Morehead City, North Carolina, USA

[5]College of Environment, Hohai University, Nanjing, China

[6]Department of Earth Sciences, Indiana University-Purdue University Indianapolis, Indianapolis, Indiana, USA

[7]University of Chinese Academy of Sciences, Beijing, China

[8]Biology Department, San Diego State University, San Diego, California, USA

[9]Estonian Marine Institute, University of Tartu, Tallinn, Estonia

[10]Nanjing Institute of Geography and Limnology, CAS, Nanjing, China

[11]Jilin Jianzhu University, Changchun, China

[12]School of Geographic Science, Changchun Normal University, Changchun, China

Correspondence
Kaishan Song, Northeast Institute of Geography and Agroecology, CAS, Changchun 130102, China.
Email: songkaishan@neigae.ac.cn

Funding information
the Youth Innovation Promotion Association of Chinese Academy of Sciences, Grant/Award Number: 2020234; Natural Science Foundation of China, Grant/Award Number: 41730104, 42071336, 42171374 and 42171385; Chinese Academy of Sciences, Grant/Award Number: YJKYYQ20190044; China Postdoctoral Science Foundation, Grant/Award Number: 2021T140662; US National Science Foundation, Grant/Award Number: 1831096 and 1840715; US National Institutes of Health, Grant/Award Number: P01ES028939

Abstract

Algal blooms (ABs) in inland lakes have caused adverse ecological effects, and health impairment of animals and humans. We used archived Landsat images to examine ABs in lakes (>1 km^2) around the globe over a 37-year time span (1982–2018). Out of the 176032 lakes with area >1 km^2 detected globally, 863 were impacted by ABs, 708 had sufficiently long records to define a trend, and 66% exhibited increasing trends in frequency ratio (FRQR, ratio of the number of ABs events observed in a year in a given lake to the number of available Landsat images for that lake) or area ratio (AR, ratio of annual maximum area covered by ABs observed in a lake to the surface area of that lake), while 34% showed a decreasing trend. Across North America, an intensification of ABs severity was observed for FRQR ($p < .01$) and AR ($p < .01$) before 1999, followed by a decrease in ABs FRQR ($p < .01$) and AR ($p < .05$) after the 2000s. The strongest intensification of ABs was observed in Asia, followed by South America, Africa, and Europe. No clear trend was detected for the Oceania. Across climatic zones, the contributions of anthropogenic factors to ABs intensification (16.5% for fertilizer, 19.4% for gross domestic product, and 18.7% for population) were slightly stronger than climatic drivers (10.1% for temperature, 11.7% for wind speed, 16.8% for pressure, and for 11.6% for

Chong Fang and Kaishan Song contributed equally to this work.

rainfall). Collectively, these divergent trends indicate that consideration of anthropogenic factors as well as climate change should be at the forefront of management policies aimed at reducing the severity and frequency of ABs in inland waters.

KEYWORDS
algal blooms, anthropogenic, climate, frequency ratio, Landsat

1 | INTRODUCTION

Globally, there are ~27 million lakes and reservoirs with an area ≥0.01 km^2, covering a total area of ~4.7 million km^2, which as a whole represent major ecological and economic resources (Pekel et al., 2016; Verpoorter et al., 2014). However, under the impact of climate change and anthropogenic perturbations, lake water quality has declined globally, as witnessed by the increased proliferation of algal blooms (ABs) in recent decades (Huang et al., 2020; Huisman et al., 2018; Paerl & Huisman, 2008; Song et al., 2021; Wurtsbaugh et al., 2019). ABs are characterized by the rapid accumulation of phytoplankton biomass, forming dense blooms (Rousso et al., 2020). Some algal taxa are capable of producing toxic compounds that lead to deteriorated quality of drinking water and recreational waters, posing a serious health threat to human and animal consumers as well as to resident aquatic organisms (Huisman et al., 2018; Paerl, 2008; Michalak et al., 2013). In September 2020, for example, more than 300 elephants in the southern African country Botswana died as a result of ingesting algal toxins (Wang et al., 2021). In addition, when ABs "crash," the decomposition of algal biomass can lead to hypoxia, a major cause of fish kills, as well as death of benthic invertebrates and loss of submerged aquatic vegetation (Chapra et al., 2017; Michalak et al., 2013; Paerl & Huisman, 2008; Paerl & Paul, 2012).

Recent studies have indicated a rise in the frequency, intensity, and duration of ABs (Burford et al., 2020; Fang et al., 2018a; Friedland et al., 2018; Kosten et al., 2012; Paerl & Huisman, 2008; Song et al., 2021). Although these have provided valuable insights into broad-scale spatiotemporal patterns of ABs in lakes, there is still an unresolved gap in our understanding of their distributional pattern at the global scale (Feng et al., 2021). This gap exists because most studies have been focused on large lakes (≥100 km^2) (Beaulieu et al., 2013; Huisman et al., 2018; Ndlela et al., 2016; Paerl & Paul, 2012), leading to limited information on smaller water bodies. Yet, these systems are more sensitive to anthropogenic and climatic pressures (Verbeek et al., 2018). Furthermore, most past studies have been confined to lakes within relatively limited geographic regions (Beaulieu et al., 2013; Duan et al., 2009; Fang et al., 2018a; Taranu et al., 2015). As a result, we lack a comprehensive understanding of the spatiotemporal patterns of lakes experiencing ABs across the globe.

Satellite imagery and ever-advancing remote sensing processing technologies facilitated time-series analysis aiming at spatiotemporal trends of ABs at various scales (Kutser, 2004, 2009; Shi et al., 2019). Data from the Landsat series are particularly well suited for ABs long-time trend analysis due to their availability over a reasonably long time period and with a higher spatial resolution (30 m) (Palmer et al., 2015).

Lakes and reservoirs are exposed to a wide range of physiochemical and biotic stressors, such as climatic change (Adrian et al., 2009; Schindler, 2009; Shi et al., 2019) and anthropogenic activities (Duan et al., 2009; Michalak et al., 2013). Nitrogen and phosphorus inputs have long been recognized as triggers for ABs in surface waters (Glibert & Burford, 2017; Huisman et al., 2018; Schindler, 1974). Some studies reported that phosphorus stimulates algal proliferation and thus is the primary nutrient of concern (Schindler and Hecky, 2008; Schindler et al., 2008; Schindler, 2012), while others have shown that nitrogen also plays an important role in controlling phytoplankton biomass along the freshwater to marine continuum (Howarth & Paerl, 2008; Lewis & Wurtsbaugh, 2008; Paerl et al., 2016, 2018; Wurtsbaugh et al., 2019). Clearly, the nutrient impacts on ABs occurrence are complex and regulated by interactions among various factors, including lake morphology, climatic conditions, hydrodynamics, and algal taxa (e.g., nitrogen-fixing vs. non-fixing) (Frenken et al., 2016; Huisman et al., 2018; Thomas et al., 2017; Rousso et al., 2020). Growing nutrient loading from urban, agricultural and industrial point and non-point sources remains the main threat to water quality and sustainable use of surface water resources (Huisman et al., 2018; Michalak et al., 2013; Winder, 2012). Factors such as fertilizer use (FRT), gross domestic product (GDP), and population growth (POP) have, respectively, been used as composite indicators of agricultural intensity, industrial output, and urban development, and identified in previous studies as the driving forces for ABs occurrence (Duan et al., 2009; Elliott, 2010; Shi et al., 2019).

Here, we exploited the imagery data from Landsat series of sensors TM/ETM+/OLI to detect and map ABs from 1982 to 2018 in lakes with an area greater than 1 km^2 across the globe (Figure S1). The study aims to (i) document the geographic distribution and temporal variations of ABs in lakes and reservoirs across the globe and (ii) quantify the contribution of anthropogenic activities and climatic factors to ABs prevalence in different climatic regions.

2 | MATERIALS AND METHODS

2.1 | Satellite images acquisition and processing

The initial satellite dataset (all lakes and reservoirs) covered 7303 path and rows (P-Rs) in the Landsat Worldwide Reference System (WRS-2), and included 863 lakes (covering 740 P-Rs) in which ABs

were detected. The total number of available Landsat images covering each AB-impacted lake (from 1982 to 2018) is reported in Figure S2 (more information about satellite images preprocessing is available in Supplementary information 1.1–1.2).

We applied three steps before retrieving ABs. First, a bulk of Landsat Level-1 GeoTIFF Data Product for the period of 1982–2018 was downloaded from the USGS Global visualization viewer website (http://glovis.usgs.gov/). Second, these images were radiometrically calibrated (based on Eq. 2 in Supplementary information 1.2). All the radiometrically calibrated images were visually inspected to check whether potential ABs appeared, true colored Red-Green-Blue images could eliminate the interference of other floating materials and organisms, such as brine shrimp (Qi et al., 2020). Furthermore, Normalized Difference Vegetation Index (NDVI) and Floating Algae Index (FAI) were calculated to identify lakes with potential ABs occurrence (Hu, 2009; Rouse et al., 1974). Third, each of the lakes with ABs were clipped using lake boundary shape files, with only one AB-impacted lake or reservoir in each outcome file.

Then, each clipped image was processed using the following steps to retrieve ABs in different lakes: (1) Batch using MNDWI to obtain the MNDWI image and selecting the best threshold for extraction of lakes/reservoirs boundary (note that the boundaries of some lakes shifted over the years or sometimes even months). This step eliminated the interference from land vegetation and floating aquatic plants. Meanwhile, Cloud was masked by setting green band threshold (Fang et al., 2018b). (2) Batch using turbid water index (TWI) to identify and eliminate the signal of turbid water (Liang et al., 2017), building a water mask to determine the portion of the image to use in the next phase of image processing. (3) Batch computing adjusted floating algae index (AFAI) images (Fang et al., 2018a, 2018b), and selection of the optimum threshold to extract AB-impacted area, and generate the corresponding files of ABs distribution (image has a corresponding optimum threshold). The AFAI method relies on the bump of NIR band in Landsat images. The above steps were executed using IDL 8.5 (Fang et al., 2018a). The expression of AFAI is as follows:

$$AFAI = R_{re,NIR} - R_{re,RED} - \left(R_{rc,SWIR} - R_{rc,RED}\right) \times 0.5 \quad (1)$$

where $R_{rc,RED}$, $R_{rc,NIR}$, and $R_{rc,SWIR}$ are the top of atmosphere reflectance of red band, near-infrared (NIR) band, and short-wave infrared (SWIR) band, respectively.

The spectral characteristics of algal blooms were significantly different from those of aquatic macrophytes in the short-wave infrared (SWIR) region, showing that the SWIR bands are crucial spectral domain for distinguishing algal blooms and aquatic macrophytes (Liang et al., 2017; Oyama et al., 2015). In this study, we applied the combination of normalized difference water index ($NDWI_{4,5}$) and the AFAI to differentiate algal blooms from aquatic macrophytes. We first used the extracted lake water surface using the method mentioned in Supplementary information 1.1, and then we used the $NDWI_{4,5}$ to classify algal blooms or aquatic macrophytes once there was an indication of potential confusion between these two types of aquatic subjects. The work of Oyama et al. (2015) has shown that the threshold of $NDWI_{4,5}$ was more robust due to its low sensitivity to remote sensing reflectance corrected by different atmospheric method. All the boundaries of ABs in each lake were visually checked to verify the accuracy. Sometimes, visual interpretation was necessary to supplement the ABs extent masked by MNDWI. Representative Landsat images observed ABs and corresponding ABs boundaries are shown in Figure S3. Finally, the final boundary, date, and area of ABs in each lake or reservoir were collected and summarized. These data were further processed or analyzed to address the study objectives.

2.2 | The definition of AR, FRQR, ABsY, AAR, and AFRQR

To investigate the spatiotemporal variation in ABs, frequency ratio (FRQR) and area ratio (AR) were computed. FRQR is the ratio of the number of ABs events observed in a year in a given lake to the number of available Landsat images for that lake. This computational approach allows to avoid ABs detection inconsistency and bias that can be introduced due to advances in remote sensing technologies over the past 40 years (Fang et al., 2018a). AR is the ratio of the maximum area covered by ABs in a year divided by the specific surface area of a lake. It is important to note that, depending on the research scale (continental, national, or climatic zone), annual FRQR was computed as the annual sum of FRQR for all AB-impacted lakes on the continent, country, or climatic zone during a given year. A similar approach was used to derive annual AR in AB-impacted lakes at these different scales. To investigate interannual trends in ABs occurrence across climatic zones, we introduced the aggregated variable ABsY, which is defined as FRQR multiplied by AR in each AB-impacted lake for every climatic region (Köppen climate classification system) (Figure S4-S7). The annual mean values of FRQR and AR were defined as AFRQR and AAR, respectively. Given the variation in lake density (hence, total lake water surface area) in different continents, countries, or regions across the world, AAR was normalized to the total amount of lake surface area in a continent, country, or region, and the ratio was reported as AAR/Area. Likewise, AFRQR was normalized to the number of AB-impacted lakes in a continent, country, or region, and the ratio reported as AFRQR/Number.

2.3 | Generation of driving forces

Multilevel analyses of the 863 ABs-impacted lakes were carried out to quantify the relative contribution of anthropogenic and climate factors. Each individual water body was regarded as an independent unit, and quantitative relationships were established between anthropogenic and climatic factors within the drainage basin associated with a specific lake. Likewise, at the climatic zone level, lakes located in the same climatic zone were aggregated and relationships with driving factors were examined across all basins within an eco-region.

The socio-economic data, including Gross Domestic Product (GDP), population (POP), fertilizer (FRT) and Nighttime Light Brightness (NTL), were computed for the catchment associated with each ABs-impacted lake (more details are available in Supplementary information 1.3). However, some of the watersheds' boundaries provided by Global Drainage Basin Database (GDBD) were too large; therefore, we generated more accurate basin boundary using GDBD, DEM, and land-use data. POP and NTL were derived directly from zonal statistics for each basin. GDP and FRT data were assembled for each administrative region. To extrapolate GDP data at the watershed level, we used population distribution as the proxy. To achieve that, we considered two scenarios: (i) catchment that covers only one country and (ii) catchment that covers two or more countries.

In the first scenario, the computation involved two steps: (1) use the zonal statistics tool in ArcGIS to obtain the population size in the watershed and (2) multiply the per-capita GDP by the number of people to derive GDP for the entire watershed. In the second scenario, the computation involved four steps: (1) use the intersect tool in ArcGIS to match each watershed boundary and the boundaries of all included countries; (2) use the zonal statistics tool in ArcGIS to obtain population number in each sub-region; (3) multiply the per-capita GDP by the number of people to derive GDP in each sub-region of the watershed; and (4) calculate GDP for the entire watershed by summing GDP of all the sub-regions.

A similar approach was adopted to calculate FRT in a watershed. In the first scenario, the computation involved three steps: (1) using the zonal statistics tool in ArcGIS, compute the cropland area in each country, and derive the average FRT per unit area of cropland; (2) using the zonal statistics tool to compute the cropland area in the watershed; (3) multiply cropland area from step 2 and FRT per cropland area (step 1) to derive FRT for the entire catchment. In the second scenario, the computation included five steps: (1) the zonal statistics tool was used to compute the cropland area in each country, and compute the average FRT per unit area of cropland; (2) the intersect tool in ArcGIS was used to match each watershed boundary and the boundaries of all included countries; (3) the zonal statistics tool was applied to obtain cropland area for each sub-region; (4) FRT for each sub-region was derived by multiplying FRT per cropland area (step 1) and cropland area in each sub-region; and (5) FRT for the entire watershed was derived by summing FRT for all the sub-regions in the watershed.

2.4 | Data analysis methods

For each of the 21 climatic zones (as well as for different seasons), mean values for both the socio-economic variables (GDP, POP, FRT, and NTL) and meteorological factors (temperature, wind speed, atmospheric pressure, and precipitation) were computed. Spearman correlation analysis was conducted using Matlab 2016a to explore relationships between anthropogenic activities and climatic elements with ABs severity in different climatic zones. When examining interannual trends in ABs at the continental and country scales, the breakpoint was determined through Mann–Kendall test (Gocic & Trajkovic, 2013; Kendall, 1948; Mann, 1945). In order to explore possible synergistic effects of anthropogenic activities and climatic elements on ABs incidence, and compare the relative importance of each forcing factor, we calculated the total adjusted R^2 and partial R^2 of all driving factors with redundancy analysis (RDA) and variation partitioning analysis (VPA). First, we used RDA to filter the most influential group of driving factors, then recomputed their separate and total contribution for each climatic zone. Second, we aggregated the identified factors into climatic and anthropogenic sub-groups, and then calculated the individual and interaction contribution of each anthropogenic and climatic factor using VPA. The interaction contribution represents the synergy between anthropogenic and climatic factors as it was accounted in both anthropogenic and climatic factors.

3 | RESULTS

3.1 | Spatiotemporal variation of lakes found ABs

ABs events were detected in 863 lakes across the globe, corresponding to a cumulative area of ~465,000 km^2, and stretching across 70 countries and regions (Figure 1). From 1982 to 2018, a total of 21,530 ABs events were documented in these lakes based on Landsat imagery analysis. Although the frequency of ABs varied among different lakes, there was a general increasing trend in annual detection of ABs globally (Figure S8), and a decreasing trend in their frequency ratio (FRQR) since 2014.

Using linear fitting, annual FRQR and AR of ABs in each lake were computed, and then we mapped the interannual change slope for these parameters (Figure 2). Out of the 863 lakes where ABs were detected, 708 had a record long enough for determining the slope of regression of FRQR and AR against time. Regardless of the confidence levels, 197 out of 708 lakes experienced synchronous increases in FRQR and AR, whereas 242 showed concomitant decreases in these parameters. Using AR or FRQR as indicators of ABs intensification, these results indicated that, over the study period, ABs occurrence was intensified in 66% of lakes (466 out 708) but decreased in 34% (242 out 708) of lakes. These results provide confirmation to speculation of global intensification of ABs in lakes (Huisman et al., 2018; Wells et al., 2015). Nevertheless, we did not find evidence of a global expansion of the geographical domain of AB-impacted lakes in neither the latitudinal nor the longitudinal direction (Table S1). Interestingly, the number of AB-impacted lakes showed a sharp decline toward the end of the record (starting in 2014) (Supplementary Dynamic Gif File, Figure S8).

Most of the lakes with ABs were distributed in high-latitude zones (latitude≥40°N) (Figure 3), and a second area with concentrated AB-impacted lakes occurred in the region between 10 and

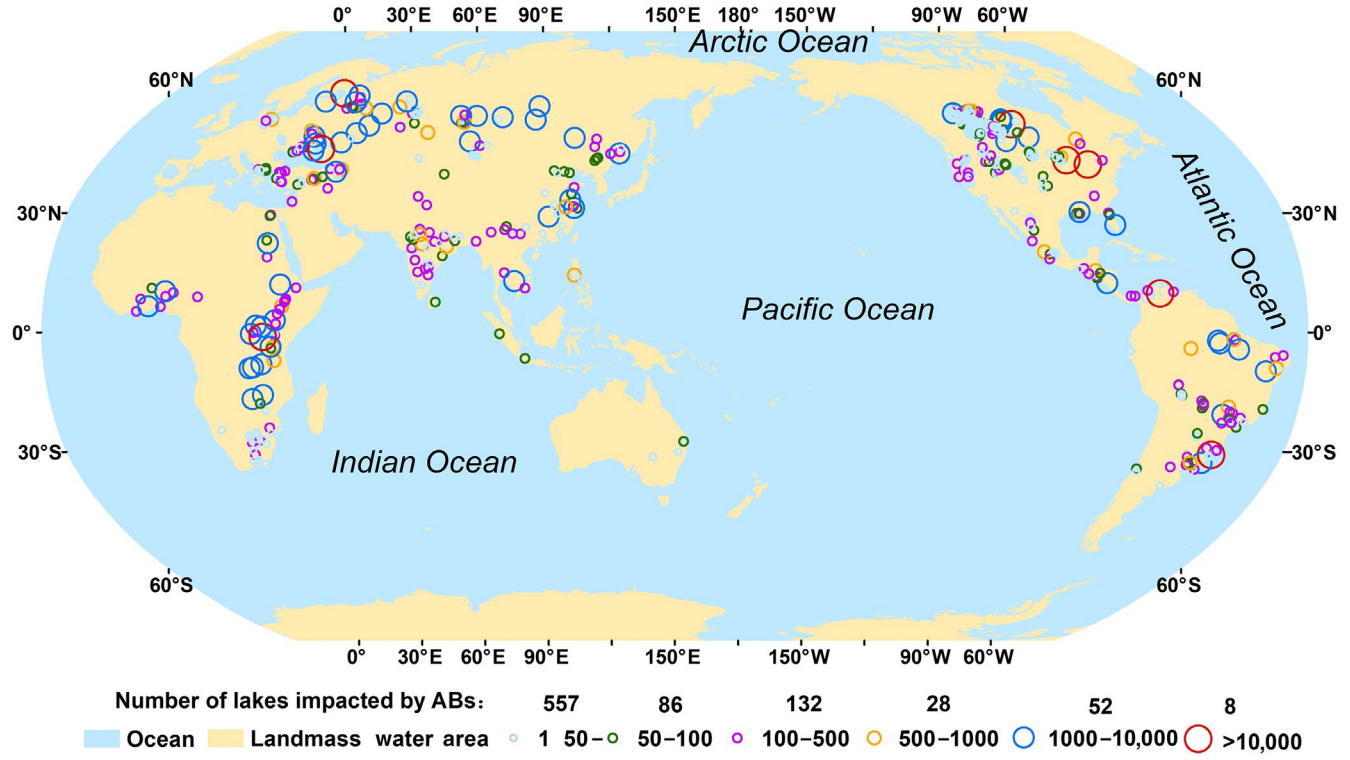

FIGURE 1 Global distribution of lakes where algal blooms (ABs) were detected. A total of 863 ABs-impacted lakes were inventoried. Based on their surface area (indicated by size of circle), lakes were distributed as follows: 1–50 km^2: 557; 50–100 km^2: 86, 100–500 km^2: 132, 500–1000 km^2: 28, 1000–10,000 km^2: 52, >10,000 km^2: 8

23.43° latitude (23.43° being the tropic line). The lakes with ABs exhibited significant increasing trends across all 10 latitude zones over the past 37 years ($p < .05$) (Figure 3b). The slope coefficients of linear regression increased with latitude in the northern hemisphere except the latitudinal zone of 10–23.43°. A similar pattern was also observed in the southern hemisphere (Figure 3).

3.2 | Continental trend in algal blooms

The distribution of ABs-impacted lakes is uneven across the globe (Figure 1). Because lake density varies greatly among the different continents (Figure S9, and Supplementary information 1.4), the parameters AFRQR and AR were normalized to total number of lakes and to total lake area, respectively (resulting parameters are AFRQR/Number and AAR/Area) to facilitate continental-scale analysis (Table S2). Based on AFRQR and AAR (Figure 4), lakes in North America and Asia experienced the highest frequency of ABs events, while Oceania exhibited the lowest. The parameters AFRQR/Number and AAR/Area were multiplied, and the product of the two indicators was used to further assess ABs severity in different continents (Table S2). Based on these criteria, the sequence of ABs severity was (from most to least) Africa, followed by South America, North America, Europe, Asia, and then Oceania.

The long-term trend of ABs in lakes of North America can be divided into two stages with 1999 being the break year (Figure 4a). From 1982 to 1999, ABs occurrence showed a significant and sustained increasing trend in both FRQR and AR ($p < .01$), while both indices decreased significantly ($p < .01$) from 2000 to 2018. These results attest to the effectiveness of phosphorus loading reduction strategies (e.g., agricultural runoff, urban wastewater discharge, P-free detergents) implemented in the United States and Canada during the last two decades (Michalak et al., 2013; Schindler, 1974). Nonetheless, there are still lakes in North America exhibiting increasing trends in FRQR (140 lakes, including 15 at a confidence level of $p < .05$; when there were only two variables in the regression, the p-value was regarded as 0) and in AR (148 lakes, including 11 at a confidence level of $p < .05$). The above-mentioned lakes are distributed throughout the North American continent (geographic location shown in Figure 2). Our observed decline in ABs occurrence since 2000 in lakes of North American was a surprising finding. Given the intensity of news coverage regarding ABs events, it is easy to think that such events are increasing in lakes across North America. Our results, however, demonstrated just the opposite trend. During the study period, lakes in Asia, Africa, and South America also showed a significant ($p < .01$) increase in both AFRQR and AAR. For lakes in Europe, the trend in ABs severity was variable and multidirectional—a peak in AFRQR and AAR in 1987 followed by a decline in 1997, and finally variable trend in AFRQR and slight intensification in AAR between 1998 and 2003. For lakes located in Oceania, ABs occurrence was detected only from 1988 to 2009, and no clear trend in AB severity was detected in the last decade.

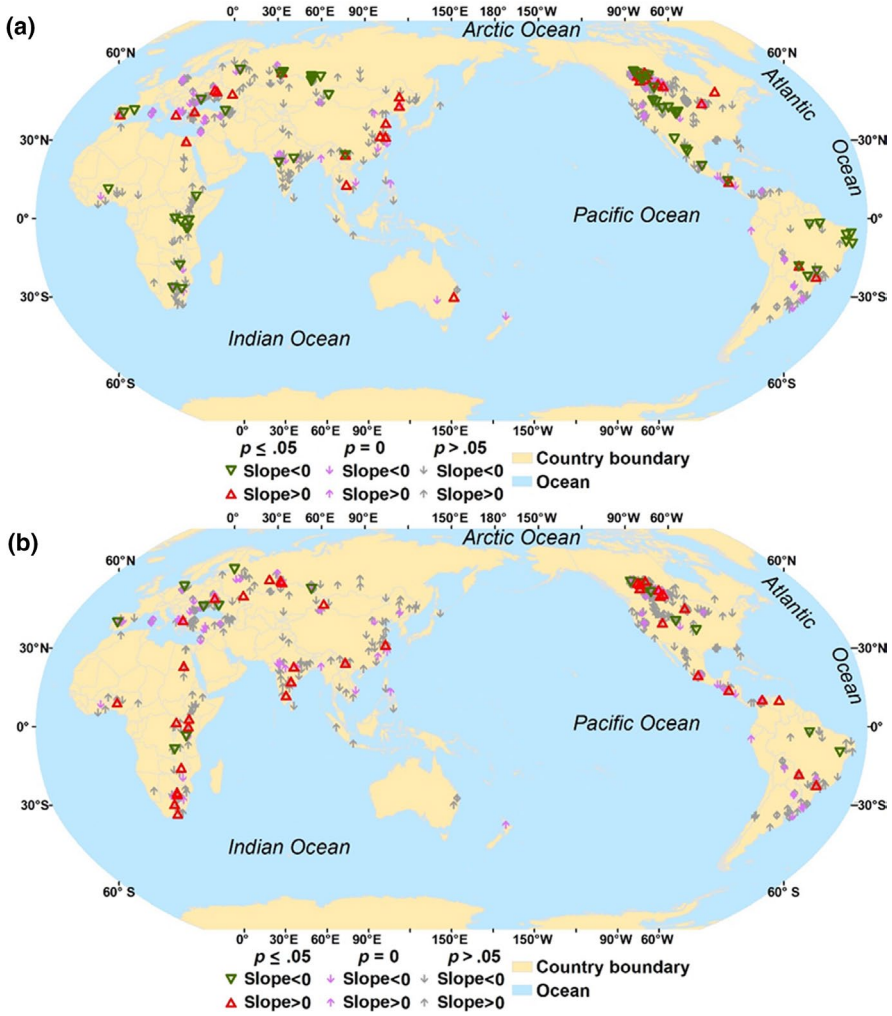

FIGURE 2 Interannual change in algal blooms (ABs) as expressed by the slope of FRQR against time (a) and AR against time (b). Slope of the temporal trend is reported for different confidence levels. FRQR is the ratio of the number of ABs events observed in a year in a given lake to the number of available Landsat images for that lake. AR is the ratio of annual maximum area covered by ABs observed in a lake to the surface area of that lake

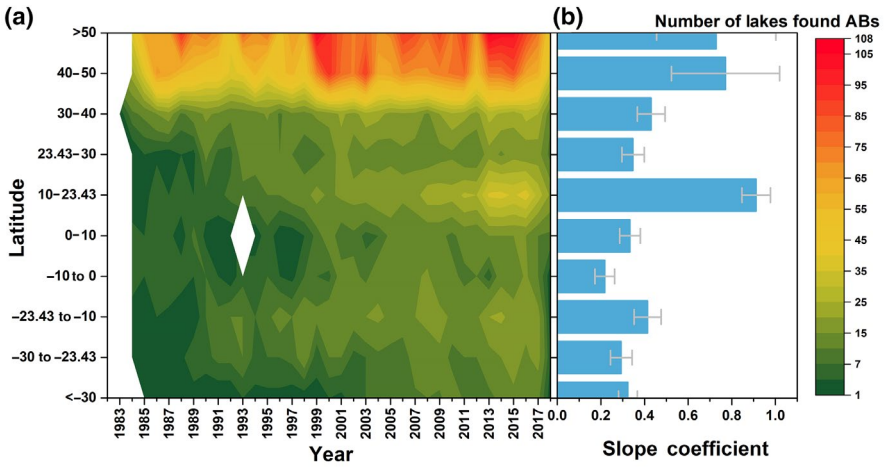

FIGURE 3 Interannual (1982–2018) changes in the number of lakes impacted by algal blooms (ABs) in different latitudes across the globe. The number of ABs-impacted lakes is shown in graph panel a, with scale to the right. The linear regression slope coefficients ($p < .05$) of the temporal trend in the Abs-impacted lakes at different latitudes are shown in panel b (blue bars), gray line represented the standard error

3.3 | Country-scale patterns in algal blooms

The country-level trends in ABs occurrence also exhibited large spatial variation globally (Figure 5a-b). The fitted linear slope of interannual trends (1982–2018) in FRQR and AR for 70 countries and regions were analyzed (Table S5-S6). To be concise, we made brief comparisons among the top 10 countries with highest frequency of ABs occurrence (Supplementary information 1.4, 1.5). Lakes in South Africa were identified as some of the most severely impacted by ABs around the world. The temporal trend of ABs in lakes of Canada can be divided into two periods—sustained and significant increase in FRQR ($p < .01$) and insignificant increase in AR ($p < .14$) from 1982 to 1999, and then decrease (although insignificant) in both parameters (FRQR, $p < .1$; AR, $p < .24$) since 2000. A similar trend was observed

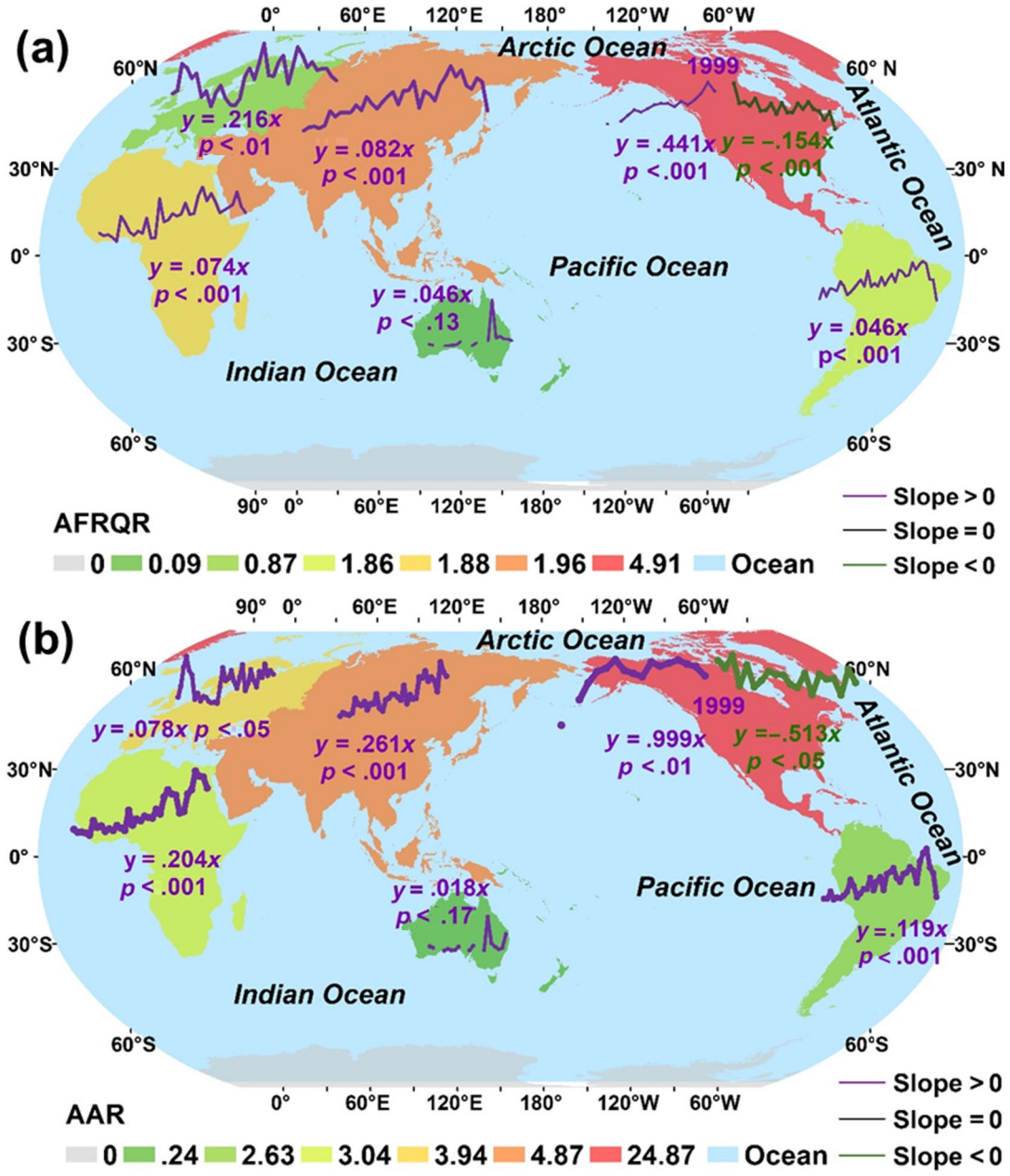

FIGURE 4 Interannual trend in algal blooms (ABs) severity across different continents from 1982 to 2018. Severity was expressed using the parameters FRQR (a) and AR (b). AFRQR is the annual mean FRQR of ABs events observed in lakes across a continent from Landsat images. Likewise, AAR is the annual mean AR of ABs observed in lakes on a continent from Landsat images. For each continent, trend line is plotted along with statistical significance of the interannual trend

in lakes of the United States—sustained significant ($p < .01$) intensification of ABs severity (as expressed by FRQR and AR) from 1982 to 1998, followed by a significant ($p < .01$) decrease in these variables between 1999 and 2018. Lakes in Brazil, Mexico, China, South Africa, and Russia showed significant ($p < .01$) increase in both FRQR and AR during the period of record (1982–2018). Overall, among the 70 countries where ABs-impacted lakes were identified, intensification of ABs was indicated in 23–26 countries based on either FRQR or AR. A decreasing trend was observed in 6 (based on AR) to 11 countries (based on FRQR).

3.4 | Variation in algal blooms along climatic zone

To examine interannual trends of ABs occurrence in different climatic zones, we introduced an aggregated variable called ABsY and defined as FRQR multiplied by AR for each lake within each of the 21 climatic regions in the Köppen climate classification system (Figure S4; Table S8). Temporal variations in FRQR, AR, and ABsY for the 21 climatic zones are presented in Figure S5-S7 (Supplementary information 1.6).

The intensifications of ABs events were noted for some climatic zones (Figure S5-S7), in coincide with global atmospheric circulation

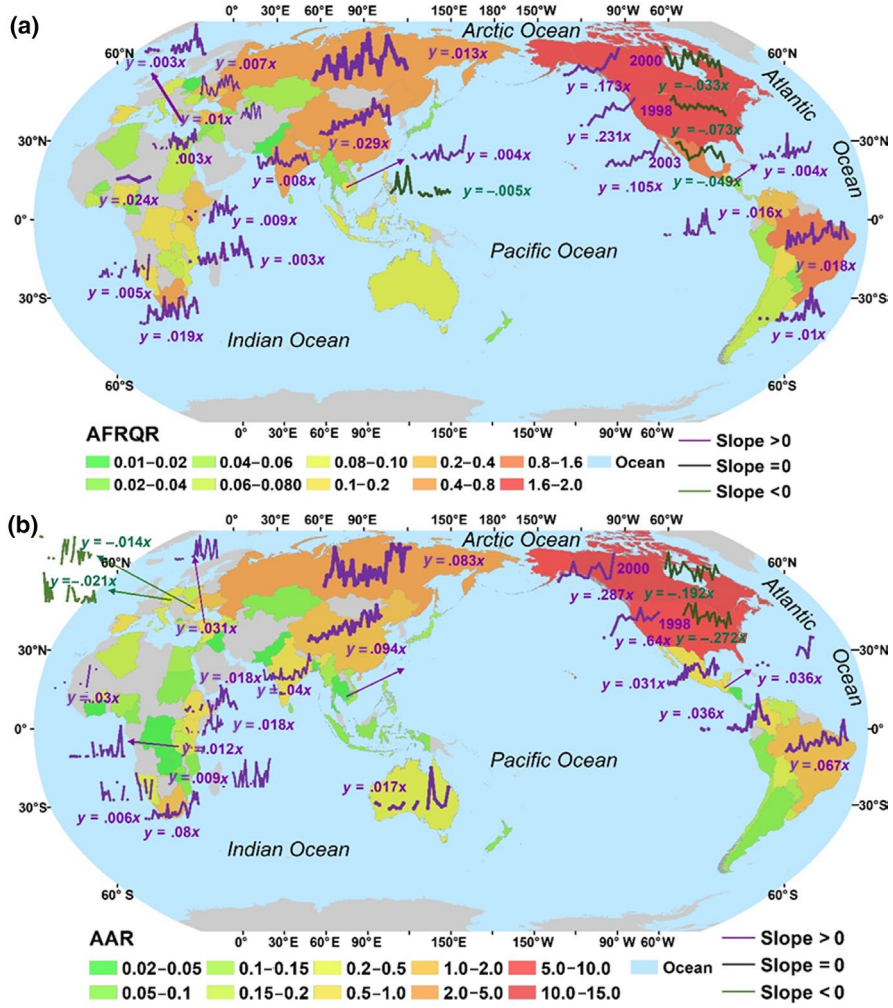

FIGURE 5 Interannual trend (1982–2018) in algal blooms (ABs) severity in selected countries. Severity was expressed using the parameters FRQR (a) and AR (b). AFRQR is the annual mean FRQR of ABs events observed in lakes across a country or region from Landsat images. Likewise, AAR is the annual mean AR of ABs observed in lakes across a country or region from Landsat images. For each country or region, trend line is plotted along with statistical significance of the interannual trend

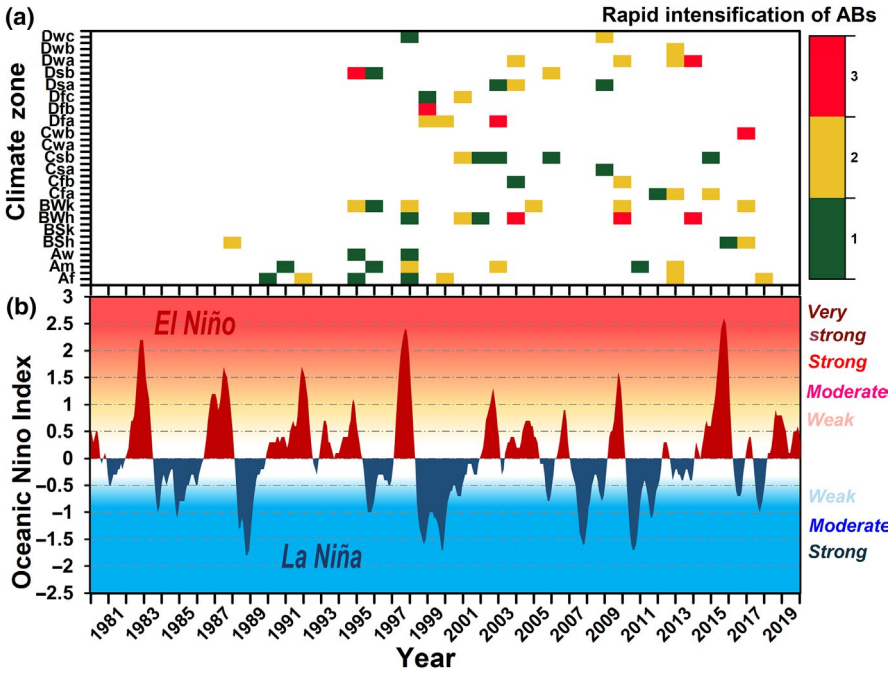

FIGURE 6 The spatiotemporal distribution of periods of rapid intensification of algal blooms (ABs) across 21 climatic zones (a), and in relation to the strength of the atmospheric circulation systems, El Niño (red) and La Niña (blue) (b). The Köppen climatic zones are described in Figure S4 and Table S8. Rapid intensification of ABs in the different climatic zones (panel a) is reported using the color code shown on the right (1 = green, 2 = yellow and 3 = red to indicate intensification based only on FRQR, only on AR, and on both FRQR and AR, respectively)

systems such as El Niño and La Nina (Figure 6). The response of lakes to these climate indices greatly varied among climatic zones (Figure 6a, Figure S5-S7). For instance, for lakes located in the Af (tropical rainforest) region, total seven times of interannual rapid intensification were identified for ABs occurrence. For lakes in the Am (tropical monsoon), BWh (tropical and subtropical desert), and

BWk (temperate desert) regions, 6 observation-years were labeled as rapid intensification, corresponding to the moderate/strong El Niño and La Niña events (Figure 6). In the other climatic zones, the influence of El Niño and La Niña events on ABs intensification was much weaker.

3.5 | Contribution of all potential factors

Analysis of the contribution of all potential climatic and anthropogenic factors to ABs severity showed that the average total adjusted R^2 of all anthropogenic (except NTL) and climatic factors was 34.98% (Figure 7). When disaggregated among the 21 climatic zones, the average contribution of climatic and anthropogenic factors was 21.44% and 24.87%, respectively. The interaction contribution of climatic and anthropogenic factors was 11.35%. Across the 21 climatic zones, the total contribution of factors varied seasonally averaging 35.42%, 38.14%, 33.37%, and 33.01% in the spring, summer, autumn, and winter, respectively (Figure 7). The contribution rates of different climate factors also showed obvious seasonal distribution differences. The effect of wind speed was more evenly distributed across the four seasons. The influence of precipitation was particularly pronounced in summer, and the effect was equal in spring and autumn. The influence of pressure was particularly prominent in spring and summer, followed by winter. The effect of temperature was most prominent in winter, with roughly similar effect during the other three seasons.

4 | DISCUSSION

4.1 | Necessity and limitation of using Landsat images

Long-term records of ABs events in lakes and reservoirs are crucial both for assessing changes in the ecological health of lacustrine ecosystems and identifying critical factors that drive these events. Yet, the availability of data for this type of analysis is often sparse, particularly in remote areas where field-based monitoring of large lakes can be exceedingly challenging (Tan et al., 2017). Fortunately, archived data from the Landsat program, the world's longest running Earth-observing satellite mission, provide a wealth of information and opportunities for uncovering evidence of past blooms (Ho et al., 2017; Woodcock et al., 2008; Wulder et al., 2012; Wynne et al., 2018). Although hyperspectral data have been used to monitor phytoplankton pigments in natural waters (Hunter et al., 2010; Matthews et al., 2010; Simis et al., 2005, 2007), to date only few studies have taken advantage of the Landsat archived data for a global-scale examination of the spatiotemporal variation of ABs in inland waters (Ho et al., 2017; Oyama et al., 2015; Song et al., 2021). In the present investigation, the long-term Landsat dataset was used to explore the spatiotemporal variation of ABs in surface waters across the globe from 1982 to 2018. It is important to note that the Landsat satellites carried different sensors at different periods of time (MSS/TM/ETM+/OLI); therefore, we examined the available images for each year and for each lake in order to minimize bias potentially arising from advances in earth observation technologies during the last four decades. Although the availability of Landsat images increased during the study period, their temporal trend was not consistent with that of FRQR and AR (Figure S8). Therefore, observed trends in FRQR and AR represent real indicators of intensification of ABs occurrence but not an artefacts resulting from greater availability of Landsat images. However, because of the relatively long revisit time of Landsat (16 days for one satellite and 8 days for two satellites at most locations) coupled with the interference of clouds, the temporal resolution of available imagery was low for some lakes. Further, because of the spatial resolution (30 m) of Landsat images, variations occurring within small blooms (e.g., buoyancy-regulating species that do not always form surface blooms; Kutser, 2004; Kutser et al., 2008) could not be detected. Thus, in light of these limitations, our results likely underestimate the true severity of ABs occurrence in some settings. With future deployments of satellites with higher temporal and spatial resolution, these limitations will likely be remedied.

4.2 | Driving forces of algal blooms intensification within climatic zones

Lakes located in climatic zones characterized by high humidity, warm/hot temperature, or extreme moisture deficit (e.g., Af, Am, BWh, BWk) seemed particularly sensitive to the effect of El Niño and La Niña (Figure 6). Therefore, consistent with previous findings for the Lake Erie region, USA (Huisman et al., 2018; Michalak et al., 2013; Paerl & Paul, 2012), global atmospheric circulation anomalies can variably impact ABs intensification depending on the climate zone.

Spearman correlations between ABsY and factors (anthropogenic, climatic) were examined (Table S9). Among the 21 climatic zones, there were 11 to 12 climatic zones in which significant ($p < .05$) correlations were found between ABsY and socio-economic factors such as GDP, POP, FRT, and NTL. Past studies have suggested similar linkages (Beaulieu et al., 2013; Michalak et al., 2013). In seven climatic zones, significant correlations were found with temperature, wind speed, pressure, and precipitation (Table S9). The results are also in accord with several past studies. Decreased wind speed was found to promote surface bloom formation (Fang et al., 2018a; Michalak et al., 2013; Rousso et al., 2020). In shallow water bodies, low to moderate disturbance caused by wind speed can lead to nutrient release due to sediment re-suspension, thereby creating conditions that fuel ABs formation (Duan et al., 2009; Michalak et al., 2013). Elevated temperature can intensify vertical stratification of the water column (Huisman et al., 2018; Paerl & Paul, 2012), and promote the growth of many motile phytoplankton species, including buoyant ABs (Beaulieu et al., 2013; Elliott, 2010; Joehnk et al., 2008; Paerl & Paul, 2012; Wagner & Adrian, 2009). Extreme weather events such as severe droughts followed by intense precipitation can also trigger ABs events through increased delivery

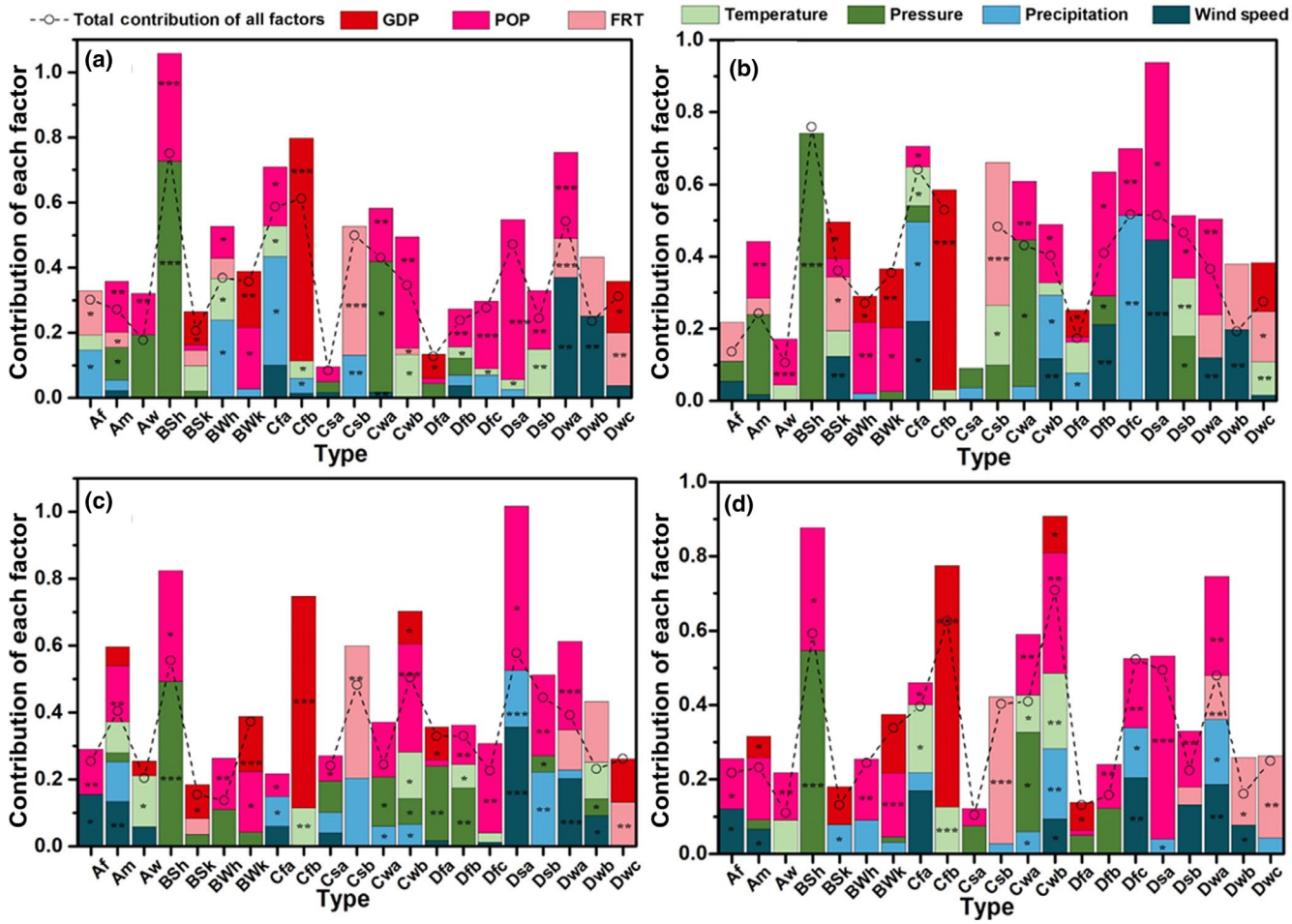

FIGURE 7 The relative and total contribution of driving factors (seven anthropogenic and climatic factors) on ABs severity in lakes based on redundancy analysis (RDA) and variation partitioning analysis (VPA). Due to the interaction, contribution was included in both anthropogenic and climatic factors, the total contribution of all factors is lower than the sum of all climatic and anthropogenic factors. Data are presented for each season: a, Spring. b, Summer. c, Autumn. d, Winter. The x-axis represent Köppen climate classification types (Figure S4; Table S8). Significance levels are indicated as "***," $p < .001$; "**," $p < .01$; and "*," $p < .05$

of nutrients from surrounding landscapes into receiving waters (Michalak et al., 2013; Paerl & Paul, 2012; Richardson et al., 2019).

For the various climatic zones, the total amount of variation in ABsY explained by anthropogenic and climatic factors was different (Figure 7). In the spring season, for example, variation in ABsY was largely explained by anthropogenic factors in 12 (out of 21) climatic zones, whereas in 9 other climatic zones variation was largely explained by climatic factors. Across all 21 climatic zones and seasons, the proportion of the total variance in ABsY explained by FRT, GDP, POP, temperature, wind speed, precipitation, atmospheric pressure, and synergy proportion by above factors averaged 16.50%, 19.43%, 18.70%, 10.14%, 11.73%, 11.65%, 16.80%, and 11.35%, respectively. Therefore, across all climatic zones, the contribution of each anthropogenic factor on ABs occurrence was on average greater than that of climatic factors (18% vs 12.5%). These results support several past studies (Glibert & Burford, 2017; Lewis & Wurtsbaugh, 2008; Paerl et al., 2020; Paerl & Paul, 2012; Raven & Geider, 1988; Thomas et al., 2017) that have documented the significance of anthropogenic factors on seasonal variation of ABs occurrence. This anthropogenic effect could be linked to increased nutrients delivery to lakes from human activities, including land-use change, alteration of landscape hydrology and increased discharge from cropland, industrial facilities, wastewater treatment plants, and sewage discharges.

4.3 | Implications for management and policymaking

Our analysis has shown that the long-term (since the 1980s) spatiotemporal variation of ABs occurrence in lakes varied in different continents, countries, and regions. Although managements have been taken to curb and reduce ABs expansion, 66% of lakes ≥1 km^2 with detected ABs exhibited increasing trends of ABs occurrence. In some developed countries and regions (e.g., North America, Europe), results have shown encouraging trends toward reversing the detrimental effects of eutrophication since the early 2000s, while in some developing regions (e.g., Asia and South America), some modest improvements have been recorded beginning in the 2010s. These trends

are strong indicators that the P and N-loading reduction strategies implemented in some regions have produced some positive effects. In contrast, in many developing countries and regions (Africa), lakes continue to experience severe ABs problems. As demonstrated by the results from North America, improvement in the lacustrine environment can be achieved through adoption of effective nutrient strategies to control eutrophication. Developing nations should aim for reduction strategies that are adapted to local socio-environmental conditions. Finally, it is important to note that, despite the success achieved during the last two decades, ABs-impacted lakes are still present in North America, underscoring the need to sustain the deployment of proven nutrients-reduction strategies until the majority of lakes in the region recover their initial ecological status. Balancing economic development and ecological sustainability is a challenging but essential goal in order to ensure long-term protection of freshwater resources for a globally expanding human population.

ACKNOWLEDGMENTS

This research was financially supported by the Natural Science Foundation of China (41730104, 42071336, 42171374, and 42171385), Research instrument and equipment development project of Chinese Academy of Sciences (YJKYYQ20190044), Project funded by the China Postdoctoral Science Foundation, China (2021T140662). Hans Paerl was supported by the US National Science Foundation, projects 1831096, 1840715, and the US National Institutes of Health (NIEHS P01ES028939). The authors thank Junbin Hou, Haiman Wu, Xinting Liu, Qingji Meng, Yang Yin, Liangyu Wang, Qiang Wang, Linwei Sha, and Shengming Li for their assistance with field sampling and laboratory analyses. Authors gratefully acknowledge the contribution of two anonymous reviewers for their constructive comments on an early version of this paper.

CONFLICT OF INTEREST

The authors declare that they have no known conflict of Interest that could have appeared to influence the work reported in this paper.

DATA AVAILABILITY STATEMENT

Landsat images were downloaded from the Earthdata Search (https://search.earthdata.nasa.gov/search) and the USGS Global visualization viewer web site (http://glovis.usgs.gov/). The GDBD was provided by the Center for Global Environmental Research (http://www.cger.nies.go.jp/db/gdbd/gdbd_index_e.html). The land-use data, from 1992 to 2015, were downloaded from the ESA GlobCover product (http://globalchange.nsdc.cn). Data pertaining to GDP and FRT in different countries and regions were downloaded from the world economic database of CEIC (https://www.ceicdata.com/zh-hans/products/global-economic-database), an extensive global database of time series data from more than 200 countries and regions, including China, the United States, and the European Union. Population (POP, 1980, 1990, 2000–2017) data were downloaded from the Netherlands Environment Assessment Agency Historical Database of the Global Environment (HYDE) (http://www.mnp.nl/hyde). The night-time light brightness (NTL) data were obtained from NOAA's National Geographic Data Center (NGDC) (https://ngdc.noaa.gov/eog/download.html). Meteorological data, including daily average temperature, precipitation, wind speed, and atmospheric pressure, were obtained from the NOAA National Meteorological Information Center (https://gis.ncdc.noaa.gov/maps/ncei). The El Niño Monitoring Indices was download from National Center for Atmospheric Research (https://climatedataguide.ucar.edu/climate-data/nino-sst-indices-nino-12-3-34-4-oni-and-tni). Other related data supporting the results could be found in supplement information and supporting data files.

ORCID

Chong Fang https://orcid.org/0000-0002-9427-0372
Kaishan Song https://orcid.org/0000-0001-9996-2450
Hans W Paerl https://orcid.org/0000-0003-2211-1011
Pierre-Andre Jacinthe https://orcid.org/0000-0002-2598-7169
Zhidan Wen https://orcid.org/0000-0002-8801-5324
Ge Liu https://orcid.org/0000-0003-1469-0690
Hui Tao https://orcid.org/0000-0002-0821-1473
Xiaofeng Xu https://orcid.org/0000-0002-6553-6514
Tiit Kutser https://orcid.org/0000-0001-9679-1422
Zongming Wang https://orcid.org/0000-0002-9865-8235
Hongtao Duan https://orcid.org/0000-0002-1985-2292
Kun Shi https://orcid.org/0000-0002-6124-7512
Yingxin Shang https://orcid.org/0000-0002-7896-2635
Lili Lyu https://orcid.org/0000-0001-8991-2644
Sijia Li https://orcid.org/0000-0003-4605-0612
Qian Yang https://orcid.org/0000-0001-8823-4175
Dongmei Lyu https://orcid.org/0000-0002-7267-7497
Dehua Mao https://orcid.org/0000-0003-3101-9153
Baohua Zhang https://orcid.org/0000-0001-8188-0190
Shuai Cheng https://orcid.org/0000-0002-9245-0628
Yunfeng Lyu https://orcid.org/0000-0002-1057-3262

REFERENCES

Adrian, R., O'Reilly, C. M., Zagarese, H., Baines, S. B., Hessen, D. O., Keller, W., Livingstone, D. M., Sommaruga, R., Straile, D., Van Donk, E., Weyhenmeyer, G. A., & Winder, M. (2009). Lakes as sentinels of climate change. *Limnology and Oceanography*, *54*, 2283–2297. https://doi.org/10.4319/lo.2009.54.6_part_2.2283

Beaulieu, M., Pick, F., & Gregory-Eaves, I. (2013). Nutrients and water temperature are significant predictors of cyanobacterial biomass in a 1147 lakes data set. *Limnology and Oceanography*, *58*, 1736–1746. https://doi.org/10.4319/lo.2013.58.5.1736

Burford, M. A., Carey, C., Hamilton, D. P., Huisman, J., Paerl, H. W., Wood, S. A., & Wulff, A. (2020). Perspective: Advancing the research agenda for improving understanding of cyanobacteria in a future of global change. *Harmful Algae*, *91*, https://doi.org/10.1016/j.hal.2019.04.004

Chapra, S. C., Boehlert, B., Fant, C., Bierman, V. J., Henderson, J., Mills, D., Mas, D. M. L., Rennels, L., Jantarasami, L., Martinich, J., Strzepek, K. M., & Paerl, H. W. (2017). Climate change impacts on harmful algal blooms in US freshwaters: A screening-level assessment. *Environmental Science and Technology*, *51*, 8933–8943. https://doi.org/10.1021/acs.est.7b01498

Duan, H., Ma, R., Xu, X., Kong, F., Zhang, S., Kong, W., Hao, J., & Shang, L. (2009). Two-decade reconstruction of algal blooms in China's Lake

Taihu. *Environmental Science & Technology*, *43*, 3522–3528. https://doi.org/10.1021/es8031852

Elliott, J. A. (2010). The seasonal sensitivity of cyanobacteria and other phytoplankton to changes in flushing rate and water temperature. *Global Change Biology*, *16*, 864–876. https://doi.org/10.1111/j.1365-2486.2009.01998.x

Fang, C., Song, K., Li, L., Wen, Z., Liu, G. E., Du, J., Shang, Y., & Zhao, Y. (2018a). Spatial variability and temporal dynamics of HABs in Northeast China. *Ecological Indicators*, *90*, 280–294. https://doi.org/10.1016/j.ecolind.2018.03.006

Fang, C., Song, K., Shang, Y., Ma, J., Wen, Z., & Du, J. (2018b). Remote sensing of harmful algal blooms variability for Lake Hulun using adjusted FAI (AFAI) algorithm. *Journal of Environmental Informatics*, https://doi.org/10.3808/jei.201700385

Feng, L., Dai, Y., Hou, X., Xu, Y., Liu, J., & Zheng, C. (2021). Concerns about phytoplankton bloom trends in global lakes. *Nature*, *590*(7846), E35-+. https://doi.org/10.1038/s41586-021-03254-3

Frenken, T., Velthuis, M., de Senerpont Domis, L. N., Stephan, S., Aben, R., Kosten, S., van Donk, E., & Van de Waal, D. B. (2016). Warming accelerates termination of a phytoplankton spring bloom by fungal parasites. *Global Change Biology*, *22*, 299–309. https://doi.org/10.1111/gcb.13095

Friedland, K. D., Mouw, C. B., Asch, R. G., Ferreira, A. S. A., Henson, S., Hyde, K. J. W., Morse, R. E., Thomas, A. C., & Brady, D. C. (2018). Phenology and time series trends of the dominant seasonal phytoplankton bloom across global scales. *Global Ecology and Biogeography*, *27*, 551–569. https://doi.org/10.1111/geb.12717

Glibert, P. M., & Burford, M. A. (2017). Globally changing nutrient loads and harmful algal blooms: Recent advances, new paradigms, and continuing challenges. *Oceanography*, *30*, 58–69. https://doi.org/10.5670/oceanog.2017.110

Gocic, M., & Trajkovic, S. (2013). Analysis of changes in meteorological variables using Mann-Kendall and Sen's slope estimator statistical tests in Serbia. *Global and Planetary Change*, *100*, 172–182. https://doi.org/10.1016/j.gloplacha.2012.10.014

Ho, J. C., Stumpf, R. P., Bridgeman, T. B., & Michalak, A. M. (2017). Using Landsat to extend the historical record of lacustrine phytoplankton blooms: A Lake Erie case study. *Remote Sensing of Environment*, *191*, 273–285. https://doi.org/10.1016/j.rse.2016.12.013

Howarth, R., & Paerl, H. W. (2008). Coastal marine eutrophication: Control of both nitrogen and phosphorus is necessary. *Proceedings of the National Academy of Sciences of the United States of America*, *105*, E103. https://doi.org/10.1073/pnas.0807266106

Hu, C. (2009). A novel ocean color index to detect floating algae in the global oceans. *Remote Sensing of Environment*, *113*(10), 2118–2129. https://doi.org/10.1016/j.rse.2009.05.012

Huang, J. C., Zhang, Y. J., Arhonditsis, G. B., Gao, J. F., Chen, Q. W., & Peng, J. (2020). The magnitude and drivers of harmful algal blooms in China's lakes and reservoirs: A national-scale characterization. *Water Research*, *181*, https://doi.org/10.1016/j.watres.2020.115902

Huisman, J., Codd, G. A., Paerl, H. W., Ibelings, B. W., Verspagen, J. M. H., & Visser, P. M. (2018). Cyanobacterial blooms. *Nature Reviews Microbiology*, *16*, 471–483. https://doi.org/10.1038/s41579-018-0040-1

Hunter, P. D., Tyler, A. N., Carvalho, L., Codd, G. A., & Maberly, S. C. (2010). Hyperspectral remote sensing of cyanobacterial pigments as indicators for cell populations and toxins in eutrophic lakes. *Remote Sensing of Environment*, *114*(11), 2705–2718. https://doi.org/10.1016/j.rse.2010.06.006

Jöhnk, K. D., Huisman, J., Sharples, J., Sommeijer, B., Visser, P. M., & Stroom, J. M. (2008). Summer heatwaves promote blooms of harmful cyanobacteria. *Global Change Biology*, *14*, 495–512. https://doi.org/10.1111/j.1365-2486.2007.01510.x

Kendall, M. (1948). *Rank correlation methods, book series, Charles Griffin*. Oxford University Press.

Kosten, S., Huszar, V. L. M., Bécares, E., Costa, L. S., Donk, E., Hansson, L.-A., Jeppesen, E., Kruk, C., Lacerot, G., Mazzeo, N., Meester, L., Moss, B., Lürling, M., Nõges, T., Romo, S., & Scheffer, M. (2012). Warmer climates boost cyanobacterial dominance in shallow lakes. *Global Change Biology*, *18*, 118–126. https://doi.org/10.1111/j.1365-2486.2011.02488.x

Kutser, T. (2004). Quantitative detection of chlorophyll in cyanobacterial blooms by satelliteremote sensing. *Limnology and Oceanography*, *49*, 2179–2189. https://doi.org/10.4319/lo.2004.49.6.2179

Kutser, T. (2009). Passive optical remote sensing of cyanobacteria and other intense phytoplankton blooms in coastal and inland waters. *International Journal of Remote Sensing*, *30*, 4401–4425. https://doi.org/10.1080/01431160802562305

Kutser, T., Metsamaa, L., & Dekker, A. G. (2008). Influence of the vertical distribution of cyanobacteria in the water column on the remote sensing signal. *Estuarine Coastal and Shelf Science*, *78*(4), 649–654. https://doi.org/10.1016/j.ecss.2008.02.024

Lewis, W. M. Jr, & Wurtsbaugh, W. A. (2008). Control of lacustrine phytoplankton by nutrients: erosion of the phosphorus paradigm. *International Review of Hydrobiology*, *93*, 446–465. https://doi.org/10.1002/iroh.200811065

Liang, Q. C., Zhang, Y. C., Ma, R. H., Loiselle, S., Li, J., & Hu, M. Q. (2017). A MODIS-based novel method to distinguish surface cyanobacterial scums and aquatic macrophytes in Lake Taihu. *Remote Sensing*, *9*(2), https://doi.org/10.3390/rs9020133

Mann, H. B. (1945). Nonparametric tests against trend. *Econometrica: Journal of the Econometric Society*, 245–259. https://doi.org/10.2307/1907187

Matthews, M. W., Bernard, S., & Winter, K. (2010). Remote sensing of cyanobacteria-dominant algal blooms and water quality parameters in Zeekoevlei, a small hypertrophic lake, using MERIS. *Remote Sensing of Environment*, *114*(9), 2070–2087. https://doi.org/10.1016/j.rse.2010.04.013

Michalak, A. M., Anderson, E. J., Beletsky, D., Boland, S., Bosch, N. S., Bridgeman, T. B., Chaffin, J. D., Cho, K., Confesor, R., Daloglu, I., DePinto, J. V., Evans, M. A., Fahnenstiel, G. L., He, L., Ho, J. C., Jenkins, L., Johengen, T. H., Kuo, K. C., LaPorte, E., … Zagorski, M. A. (2013). Record-setting algal bloom in Lake Erie caused by agricultural and meteorological trends consistent with expected future conditions. *Proceedings of the National Academy of Sciences of the United States of America*, *110*, 6448–6452. https://doi.org/10.1073/pnas.1216006110

Ndlela, L. L., Oberholster, P. J., Van Wyk, J. H., & Cheng, P. H. (2016). An overview of cyanobacterial bloom occurrences and research in Africa over the last decade. *Harmful Algae*, *60*, 11–26. https://doi.org/10.1016/j.hal.2016.10.001

Oyama, Y., Matsushita, B., & Fukushima, T. (2015). Distinguishing surface cyanobacterial blooms and aquatic macrophytes using Landsat/TM and ETM+ shortwave infrared bands. *Remote Sensing of Environment*, *157*, 35–47. https://doi.org/10.1016/j.rse.2014.04.031

Paerl, H. (2008). Nutrient and other environmental controls of harmful cyanobacterial blooms along the freshwater–marine continuum. In *Cyanobacterial harmful algal blooms: state of the science and research needs* (pp. 217–237). Springer.

Paerl, H. W. (2009). Controlling eutrophication along the freshwater–marine continuum: Dual nutrient (N and P) reductions are essential. *Estuaries and Coasts*, *32*, 593–601. https://doi.org/10.1007/s12237-009-9158-8

Paerl, H. W., Havens, K. E., Hall, N. S., Otten, T. G., Zhu, M., Xu, H., Zhu, G., & Qin, B. (2020). Mitigating a global expansion of toxic cyanobacterial blooms: Confounding effects and challenges posed by climate change. *Marine and Freshwater Research*, *71*(5), 579–592. https://doi.org/10.1071/mf18392

Paerl, H. W., & Huisman, J. (2008). Blooms like it hot. *Science*, *320*, 57–58. https://doi.org/10.1126/science.1155398

Paerl, H. W., & Huisman, J. (2009). Climate change: A catalyst for global expansion of harmful cyanobacterial blooms. *Environmental Microbiology Reports*, *1*, 27–37. https://doi.org/10.1111/j.1758-2229.2008.00004.x

Paerl, H. W., Otten, T. G., & Kudela, R. (2018). Mitigating the expansion of harmful algal blooms across the freshwater-to-marine continuum. *Environmental Science and Technology*, *52*(10), 5519–5529. https://doi.org/10.1021/acs.est.7b05950

Paerl, H. W., & Paul, V. J. (2012). Climate change: links to global expansion of harmful cyanobacteria. *Water Research*, *46*, 1349–1363. https://doi.org/10.1016/j.watres.2011.08.002

Paerl, H. W., Scott, J. T., McCarthy, M. J., Newell, S. E., Gardner, W. S., Havens, K. E., & Wurtsbaugh, W. A. (2016). It takes two to tango: When and where dual nutrient (N & P) reductions are needed to protect lakes and downstream ecosystems. *Environmental Science and Technology*, *50*(20), 10805–10813. https://doi.org/10.1021/acs.est.6b02575

Palmer, S. C., Kutser, T., & Hunter, P. D. (2015). Remote sensing of inland waters: Challenges, progress and future directions. *Remote Sensing of Environment*, Elsevier, *157*, 1–8. https://doi.org/10.1016/j.rse.2014.09.021

Pekel, J. F., Cottam, A., Gorelick, N., & Belward, A. S. (2016). High-resolution mapping of global surface water and its long-term changes. *Nature*, *540*, 418–422. https://doi.org/10.1038/nature20584

Qi, L., Hu, C., Mikelsons, K., Wang, M., Lance, V., Sun, S., Barnes, B. B., Zhao, J., & Van der Zande, D. (2020). In search of floating algae and other organisms in global oceans and lakes. *Remote Sensing of Environment*, *239*, 111659. https://doi.org/10.1016/j.rse.2020.111659s

Raven, J. A., & Geider, R. J. (1988). Temperature and algal growth. *New Phytologist*, *110*, 441–461. https://doi.org/10.1111/j.1469-8137.1988.tb00282.x

Richardson, J., Feuchtmayr, H., Miller, C., Hunter, P. D., Maberly, S. C., & Carvalho, L. (2019). Response of cyanobacteria and phytoplankton abundance to warming, extreme rainfall events and nutrient enrichment. *Global Change Biology*, *25*(10), 3365–3380. https://doi.org/10.1111/gcb.14701

Rouse, J., Haas, R., Schell, J., & Deering, D. (1974). Monitoring vegetation systems in the Great Plains with ERTS. *NASA Special Publication*, *351*, 309.

Rousso, B. Z., Bertone, E., Stewart, R., & Hamilton D. P. (2020). A systematic literature review of forecasting and predictive models for cyanobacteria blooms in freshwater lakes. *Water Research*, *182*, 115959. https://doi.org/10.1016/j.watres.2020.115959

Schindler, D. W. (1974). Eutrophication and recovery in experimental lakes: Implications for lake management. *Science*, *184*, 897–899. https://doi.org/10.1126/science.184.4139.897

Schindler, D. (2009). Lakes as sentinels and integrators for the effects of climate change on watersheds, airsheds, and landscapes. *Limnology and Oceanography*, *54*, 2349–2358. https://doi.org/10.4319/lo.2009.54.6_part_2.2349

Schindler, D. W. (2012). The dilemma of controlling cultural eutrophication of lakes. *Proceedings of the Royal Society B: Biological Sciences*, *279*, 4322–4333. https://doi.org/10.1098/rspb.2012.1032

Schindler, D., & Hecky, R. (2008). Reply to Howarth and Paerl: Is control of both nitrogen and phosphorus necessary? *Proceedings of the National Academy of Sciences of the United States of America*, *105*, E104. https://doi.org/10.1073/pnas.0809744105

Schindler, D. W., Hecky, R. E., Findlay, D. L., Stainton, M. P., Parker, B. R., Paterson, M. J., Beaty, K. G., Lyng, M., & Kasian, S. E. M. (2008). Eutrophication of lakes cannot be controlled by reducing nitrogen input: Results of a 37-year whole-ecosystem experiment. *Proceedings of the National Academy of Sciences of the United States of America*, *105*, 11254–11258. https://doi.org/10.1073/pnas.0805108105

Shi, K., Zhang, Y., Zhang, Y., Li, N. A., Qin, B., Zhu, G., & Zhou, Y. (2019). Phenology of phytoplankton blooms in a trophic lake observed from long-term MODIS data. *Environmental Science and Technology*, *53*(5), 2324–2331. https://doi.org/10.1021/acs.est.8b06887

Simis, S. G., Peters, S. W., & Gons, H. J. (2005). Remote sensing of the cyanobacterial pigment phycocyanin in turbid inland water. *Limnology and Oceanography*, *50*(1), 237–245. https://doi.org/10.4319/lo.2005.50.1.0237

Simis, S. G. H., Ruiz-Verdu, A., Dominguez-Gomez, J. A., Pena-Martinez, R., Peters, S. W. M., & Gons, H. J. (2007). Influence of phytoplankton pigment composition on remote sensing of cyanobacterial biomass. *Remote Sensing of Environment*, *106*(4), 414–427. https://doi.org/10.1016/j.rse.2006.09.008

Song, K., Fang, C., Jacinthe, P.-A., Wen, Z., Liu, G., Xu, X., Shang, Y., & Lyu, L. (2021). Climatic versus anthropogenic controls of decadal trends (1983–2017) in algal blooms in lakes and reservoirs across China. *Environmental Science and Technology*, *55*(5), 2929–2938. https://doi.org/10.1021/acs.est.0c06480

Tan, W., Liu, P., Liu, Y., Yang, S., & Feng, S. (2017). A 30-year assessment of phytoplankton blooms in Erhai Lake using Landsat imagery: 1987 to 2016. *Remote Sensing*, *9*(12), 1265. https://doi.org/10.3390/rs9121265

Taranu, Z. E., Gregory-Eaves, I., Leavitt, P. R., Bunting, L., Buchaca, T., Catalan, J., Domaizon, I., Guilizzoni, P., Lami, A., McGowan, S., Moorhouse, H., Morabito, G., Pick, F. R., Stevenson, M. A., Thompson, P. L., & Vinebrooke, R. D. (2015). Acceleration of cyanobacterial dominance in north temperate-subarctic lakes during the Anthropocene. *Ecology Letters*, *18*, 375–384. https://doi.org/10.1111/ele.12420

Thomas, M. K., Aranguren-Gassis, M., Kremer, C. T., Gould, M. R., Anderson, K., Klausmeier, C. A., & Litchman, E. (2017). Temperature-nutrient interactions exacerbate sensitivity to warming in phytoplankton. *Global Change Biology*, *23*, 3269–3280. https://doi.org/10.1111/gcb.13641

Verbeek, L., Gall, A., Hillebrand, H., & Striebel, M. (2018). Warming and oligotrophication cause shifts in freshwater phytoplankton communities. *Global Change Biology*, *24*, 4532–4543. https://doi.org/10.1111/gcb.14337

Verpoorter, C., Kutser, T., Seekell, D. A., & Tranvik, L. J. (2014). A global inventory of lakes based on high-resolution satellite imagery. *Geophysical Research Letters*, *41*(18), 6396–6402. https://doi.org/10.1002/2014GL060641

Wagner, C., & Adrian, R. (2009). Cyanobacteria dominance: Quantifying the effects of climate change. *Limnology and Oceanography*, *54*, 2460–2468. https://doi.org/10.4319/lo.2009.54.6_part_2.2460

Wang, H., Xu, C., Liu, Y., Jeppesen, E., Svenning, J.-C., Wu, J., … Xie, P. (2021). From unusual suspect to serial killer: Cyanotoxins boosted by climate change may jeopardize megafauna. *Innovation*, *2*(2), 100092. https://doi.org/10.1016/j.xinn.2021.100092

Wells, M. L., Trainer, V. L., Smayda, T. J., Karlson, B. S. O., Trick, C. G., Kudela, R. M., Ishikawa, A., Bernard, S., Wulff, A., Anderson, D. M., & Cochlan, W. P. (2015). Harmful algal blooms and climate change: Learning from the past and present to forecast the future. *Harmful Algae*, *49*, 68–93. https://doi.org/10.1016/j.hal.2015.07.009

Winder, M. (2012). Limnology: Lake warming mimics fertilization. *Nature Climate Change*, *2*, 771–772. https://doi.org/10.1038/nclimate1728

Woodcock, C. E., Allen, R., Anderson, M., Belward, A., Bindschadler, R., Cohen, W., Gao, F., Goward, S., Helder, D., & Helmer, E. (2008). Free access to Landsat imagery. *Science*, *320*(5879), 1011.

Wulder, M. A., Masek, J. G., Cohen, W. B., Loveland, T. R., & Woodcock, C. E. (2012). Opening the archive: How free data has enabled the science and monitoring promise of Landsat. *Remote Sensing of Environment*, *122*, 2–10. https://doi.org/10.1016/j.rse.2012.01.010

Wurtsbaugh, W. A., Paerl, H. W., & Dodds, W. K. (2019). Nutrients, eutrophication and harmful algal blooms along the freshwater to marine

continuum. *Wiley Interdisciplinary Reviews-Water*, *6*(5), https://doi.org/10.1002/wat2.1373

Wynne, T., Meredith, A., Briggs, T., Litaker, W., & Stumpf, R. (2018). *Harmful algal bloom forecasting branch ocean color satellite imagery processing guidelines*. NOAA Technical Memorandum NOS NCCOS, *252*, 3. https://doi.org/10.25923/twc0-f025

SUPPORTING INFORMATION

Additional supporting information may be found in the online version of the article at the publisher's website.

How to cite this article: Fang, C., Song, K., Paerl, H. W., Jacinthe, P.-A., Wen, Z., Liu, G., Tao, H., Xu, X., Kutser, T., Wang, Z., Duan, H., Shi, K., Shang, Y., Lyu, L., Li, S., Yang, Q., Lyu, D., Mao, D., Zhang, B., … Lyu, Y. (2022). Global divergent trends of algal blooms detected by satellite during 1982–2018. *Global Change Biology*, 00, 1–14. https://doi.org/10.1111/gcb.16077